2013

Epidemics in Adaptive Social Networks with Temporary Link Deactivation

Ilker Tunc
William & Mary

Leah B. Shaw
William & Mary, lbshaw@wm.edu

Maxim S. Shkarayev

Recommended Citation

Tunc, I., Shkarayev, M. S., & Shaw, L. B. (2013). Epidemics in adaptive social networks with temporary link deactivation. Journal of statistical physics, 151(1-2), 355-366.

J Stat Phys (2013) 151:355–366
DOI 10.1007/s10955-012-0667-7

Epidemics in Adaptive Social Networks with Temporary Link Deactivation

Ilker Tunc · Maxim S. Shkarayev · Leah B. Shaw

Received: 1 August 2012 / Accepted: 4 December 2012 / Published online: 19 December 2012

Abstract Disease spread in a society depends on the topology of the network of social contacts. Moreover, individuals may respond to the epidemic by adapting their contacts to reduce the risk of infection, thus changing the network structure and affecting future disease spread. We propose an adaptation mechanism where healthy individuals may choose to temporarily deactivate their contacts with sick individuals, allowing reactivation once both individuals are healthy. We develop a mean-field description of this system and find two distinct regimes: slow network dynamics, where the adaptation mechanism simply reduces the effective number of contacts per individual, and fast network dynamics, where more efficient adaptation reduces the spread of disease by targeting dangerous connections. Analysis of the bifurcation structure is supported by numerical simulations of disease spread on an adaptive network. The system displays a single parameter-dependent stable steady state and non-monotonic dependence of connectivity on link deactivation rate.

Keywords Adaptive network · Dynamical network · SIS model · Link deactivation

1 Introduction

In classical compartmental epidemic models, it is assumed that the population is homogeneously mixed, and every individual has an equal chance to contact any other individual in the population [2]. As this assumption is relaxed, the social network topology is included [1, 8, 13]. Furthermore, disease spread on both static [11, 12, 14, 15] and evolving [18, 21] networks are considered.

A class of epidemic models that recently has received a lot of attention considers the situation where people may change their social preferences during an epidemic to avoid exposure to disease [5, 17]. These models try to take into account the effect that the presence

I. Tunc (✉) · L.B. Shaw
Department of Applied Science, College of William and Mary, Williamsburg, VA 23187, USA
e-mail: itunc@email.wm.edu

M.S. Shkarayev
Department of Physics & Astronomy, Iowa State University, Ames, IA 50011, USA

of the disease can have on the network topology. The individuals in the society may choose to adapt their local connections based on the desire to quarantine themselves from the epidemic. This in turn affects the further spread of the disease. Some models consider rewiring of potentially dangerous connections as the adaptation mechanism [6, 16, 19, 24]. That is, when a contact between individuals is abandoned, a new contact is immediately formed, and the total number of connections is conserved. A motivation for these models is that social connections serve a purpose, and thus a fixed number of connections must be maintained for society to continue functioning. In the first models of this type, a healthy individual breaks its connection with a sick individual, in favor of some other healthy individual [6, 19]. The assumption in this model is that each person knows the infection status of all the people in the society. In [24], relaxing this assumption, a healthy person reconnects to a randomly chosen person. Furthermore, sick individuals may altruistically rewire their links away from their healthy contacts [16]. With rewiring as the adaptation mechanism, bistability is frequently observed, where both the disease free state and endemic state coexist for some range of parameters.

Other adaptation mechanisms that have been studied do not preserve the total number of connections in the society. Jolad et al. studies networks in which connections are created and abandoned in an attempt to achieve some preferred number of connections [7]. In this case, the adaptation mechanism reduces the expected number of contacts between the individuals as a response to the global infection prevalence, which in turn reduces the spread of infection. Zhou et al. considers growing networks in which connections between healthy and sick nodes are deleted, with the constraint that nodes can not be completely isolated [25]. In this case, the combination of network growth, connection removal, and isolation avoidance lead to recurring epidemic outbreaks. Kiss et al. studies an adaptive network in which the connections are abandoned or created at rates dependent on the status of individuals [10]. Here a variety of bifurcation structures, including bistable solutions, are observed.

We expect that in real social networks, people tend to avoid contact with their infected neighbors during an epidemic. However, once an infected neighbor recovers, people would resume social relations with that neighbor. This is in contrast to previous models in which social connections are deleted or rewired away in response to an infection, never to be resumed. In order to study this type of social behavior, we consider an adaptive network model where a susceptible node temporarily deletes or deactivates links to its infected neighbors. It then recreates or reactivates these links after its neighbors have recovered. In our model, link deletion and creation are constrained in that link creation is only allowed for the previously deleted links. There is an overarching static network structure of all possible links that could exist, and the neighborhood of each node is preserved. We assume a complex network structure rather than the complete network geometry used in [10]. Results are presented here for Erdős-Rényi random networks [3], but the approach can be used for any other complex (and potentially more realistic) network geometry. In a related model by Valdez et al., connections between susceptible and infected nodes are temporarily interrupted [23]. The period over which the connection is deactivated is shorter than the infectious period of the disease, and a connection might be interrupted and restored several times before the infected node recovered. However, because people can communicate their infection status without in-person contact (e.g., by telephone), we will assume that nodes know the infection status of their neighbors and do not reactivate connections until their neighbors have recovered. In particular, unlike [10, 23], we do not allow links between susceptibles and infectives to be activated.

In Sect. 2, we specify the model dynamics. In Sect. 3, we present a mean-field analytic approach and argue that bistability does not occur with our adaptation mechanism, in contrast

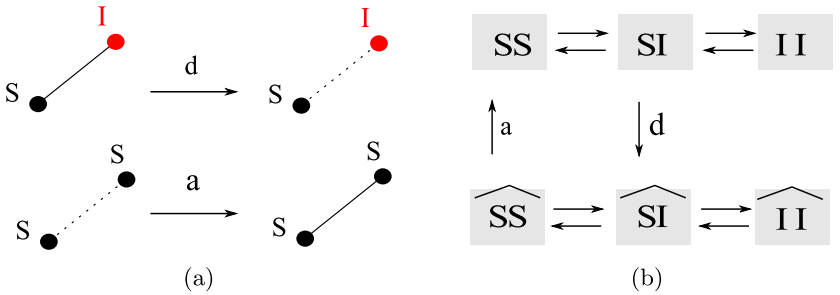

Fig. 1 (**a**) Schematic of the adaptation mechanism. An active SI link is deactivated with deactivation rate d, and a deactivated SS link is reactivated with reactivation rate a. (**b**) Schematic of the link dynamics in the network. Horizontal arrows indicate infection (*arrows toward right*) and recovery (*arrows toward left*) transitions

to many models with rewiring adaptation. In Sect. 4, we present stochastic and mean-field results for infection levels and for the geometry of the active subnetwork. We conclude and discuss future applications in Sect. 5.

2 Model

We study epidemic spread in a population that is represented by a network. Disease spread is modeled by using a susceptible-infected-susceptible (SIS) dynamics on the network [2]. In this model, individuals can be in one of two states: *infected* with the disease and contagious (I), or healthy and *susceptible* to the infection (S). The disease can spread via contact between susceptibles and infectives at a constant infection rate p per SI link. The infected individuals recover from the disease, becoming susceptible again, at a constant recovery rate r.

We allow healthy individuals to adapt their relationships so as to reduce the risk of being infected. In this model, susceptible individuals know the infection status of all their neighbors and can temporarily deactivate their connections to infected neighbors, a process that takes place at a deactivation rate d. Once both individuals are susceptible, the deactivated links are reactivated at a reactivation rate a. The deactivation and reactivation processes are illustrated in Fig. 1(a). Note that these processes take place on an unchanging network: what changes is its active part, i.e., the subset of links that allow the disease transmission.

We study the dynamics of the disease spread on a network with a fixed number of nodes, N, and a fixed number of links, K. The average degree of the network, κ, is then given by $\kappa = 2K/N$. Given an initial network geometry, the node and network dynamics are simulated using a continuous time Monte Carlo algorithm [4]. Simulation results presented in this paper are for Erdős-Rényi networks [3] with $N = 10^4$ and $K = 10^5$ unless otherwise specified. Self-links and multiple links between nodes are not allowed.

3 Analytical Approach

In this section, we approximate the full system using a mean-field approach [6, 9]. The following system of equations describes the evolution of the number of each type of node:

$$\frac{dN_{\mathrm{S}}}{dt} = rN_{\mathrm{I}} - pN_{\mathrm{SI}}, \tag{1a}$$

$$\frac{dN_{\mathrm{I}}}{dt} = -rN_{\mathrm{I}} + pN_{\mathrm{SI}}, \tag{1b}$$

and each type of link:

$$\frac{dN_{\mathrm{SS}}}{dt} = rN_{\mathrm{SI}} - pN_{\mathrm{SSI}} + aN_{\widehat{\mathrm{SS}}}, \tag{2a}$$

$$\frac{dN_{\mathrm{SI}}}{dt} = r(2N_{\mathrm{II}} - N_{\mathrm{SI}}) + p(N_{\mathrm{SSI}} - N_{\mathrm{ISI}}) - dN_{\mathrm{SI}}, \tag{2b}$$

$$\frac{dN_{\mathrm{II}}}{dt} = -2rN_{\mathrm{II}} + pN_{\mathrm{ISI}} \tag{2c}$$

$$\frac{dN_{\widehat{\mathrm{SS}}}}{dt} = rN_{\widehat{\mathrm{SI}}} - pN_{\widehat{\mathrm{SS}}\mathrm{I}} - aN_{\widehat{\mathrm{SS}}}, \tag{2d}$$

$$\frac{dN_{\widehat{\mathrm{SI}}}}{dt} = r(2N_{\widehat{\mathrm{II}}} - N_{\widehat{\mathrm{SI}}}) + p(N_{\widehat{\mathrm{SS}}\mathrm{I}} - N_{\widehat{\mathrm{IS}}\mathrm{I}}) + dN_{\mathrm{SI}}, \tag{2e}$$

$$\frac{dN_{\widehat{\mathrm{II}}}}{dt} = -2rN_{\widehat{\mathrm{II}}} + pN_{\widehat{\mathrm{IS}}\mathrm{I}}, \tag{2f}$$

where N_{X} denotes the expected number of nodes in state X, while N_{XY} and $N_{\widehat{\mathrm{XY}}}$ respectively denote the expected number of active and deactivated links connecting nodes in states X and Y, with $\mathrm{X} \in \{\mathrm{S}, \mathrm{I}\}$. The notation N_{XYZ} denotes the expected number of triples of connected nodes of type X, Y, and Z, with a circumflex over nodes that are connected by a deactivated link. Note that our definition of an XYX type of a triple includes the degenerate triples, i.e., those triples formed by a Y-node and a single X-node. Equations (1a), (1b) reflect the transitions of nodes between susceptible and infected states, while Eqs. (2a)–(2f) reflect the link transitions indicated in Fig. 1(b). The values of N_{X}, N_{XY} and $N_{\widehat{\mathrm{XY}}}$ are treated as continuous in the limit of large network size.

The system of Eqs. (1a), (1b) and (2a)–(2f) is open since it contains unknown quantities corresponding to the statistics of the higher order node formations, i.e., the number of connected triples of nodes where at least one of the links is of SI type. Thus, in order to close the system, we approximate the number of triples in the system using the moment closure approximation discussed in [6, 9, 20]:

$$N_{\mathrm{XSI}} = \frac{2N_{\mathrm{XS}}}{N_{\mathrm{S}}}\frac{N_{\mathrm{SI}}}{N_{\mathrm{S}}}N_{\mathrm{S}} \quad \text{for } \mathrm{XS} \in \{\mathrm{SS}, \widehat{\mathrm{SS}}\} \tag{3a}$$

$$N_{\widehat{\mathrm{IS}}\mathrm{I}} = \frac{N_{\widehat{\mathrm{SI}}}}{N_{\mathrm{S}}}\frac{N_{\mathrm{SI}}}{N_{\mathrm{S}}}N_{\mathrm{S}} \tag{3b}$$

$$N_{\mathrm{ISI}} = \left(\left(\frac{N_{\mathrm{SI}}}{N_{\mathrm{S}}}\right)^2 + \frac{N_{\mathrm{SI}}}{N_{\mathrm{S}}}\right)N_{\mathrm{S}}. \tag{3c}$$

This closure corresponds to the assumption that, if one follows a link that stems from a susceptible node, the probability that a node at the end of that link is infected is independent of any other information available about that susceptible node.

In order to simplify the analysis, we set $r = 1$, which is equivalent to rescaling the time by $1/r$. We also rescale the quantities N_{X} and N_{XY} by N and K respectively. Since both the total number of nodes and the total number of links are conserved, the quantities $P_{\mathrm{X}} \equiv N^{-1}N_{\mathrm{X}}$ and $P_{\mathrm{XY}} \equiv K^{-1}N_{\mathrm{XY}}$ correspond to the fraction of the nodes of type X and fraction of links of type XY respectively.

Using conservation of nodes, we can eliminate one of the node equations in (1a), (1b). Similarly, using conservation of links, we can eliminate one of the equations in (2a)–(2f). Thus, the state of the full system is approximated by the vector $\mathbf{x} = (P_{\mathrm{I}}, P_{\mathrm{SS}}, P_{\mathrm{SI}}, P_{\mathrm{II}}, P_{\widehat{\mathrm{SS}}}, P_{\widehat{\mathrm{SI}}})$. Note that the remaining two quantities, P_{S} and $P_{\widehat{\mathrm{II}}}$, are found from the equations for conservation of nodes and links: $P_{\mathrm{S}} = 1 - P_{\mathrm{I}}$ and $P_{\widehat{\mathrm{II}}} = 1 - P_{\mathrm{SS}} - P_{\mathrm{SI}} - P_{\mathrm{II}} - P_{\widehat{\mathrm{SS}}} - P_{\widehat{\mathrm{SI}}}$.

This system has a unique disease-free state (DFS) given by the vector $\mathbf{x_0} = (0, 1, 0, 0, 0, 0)$ for $a \neq 0$. We analyze the stability of the disease-free state by evaluating the Jacobian at the DFS:

$$\mathbf{J}|_{\mathbf{x_0}} = \begin{pmatrix} -1 & 0 & \frac{p\kappa}{2} & 0 & 0 & 0 \\ 0 & 0 & 1 - p\kappa & 0 & a & 0 \\ 0 & 0 & -1 - p - d + p\kappa & 2 & 0 & 0 \\ 0 & 0 & p & -2 & 0 & 0 \\ 0 & 0 & 0 & 0 & -a & 1 \\ 0 & -2 & d - 2 & -2 & -2 & -3 \end{pmatrix}.$$

In order for the DFS to be stable, the real part of the eigenvalues of the Jacobian must be less than zero. Four of the eigenvalues of the Jacobian are $\lambda_1 = -1$, $\lambda_2 = -1$, $\lambda_3 = -2$, $\lambda_4 = -a$, all of which are less than zero. The remaining two eigenvalues λ_5 and λ_6 are given as the solutions to the equation:

$$\lambda^2 + \lambda\big((d + 1 - p\kappa) + 2 + p\big) + 2(d + 1 - p\kappa) = 0.$$

We note that if $d + 1 - p\kappa > 0$ then (i) $\lambda_5\lambda_6 = 2(d + 1 - p\kappa) > 0$ and (ii) $\lambda_5 + \lambda_6 = -((d + 1 - p\kappa) + 2 + p) < 0$. If both (i) and (ii) hold, then both $\mathrm{Re}(\lambda_5) < 0$ and $\mathrm{Re}(\lambda_6) < 0$, and therefore the DFS must be locally stable for $p < (d + 1)/\kappa$. On the other hand, the relation $\lambda_5\lambda_6 = d + 1 - p\kappa < 0$ implies that one of the eigenvalues is positive and the DFS loses stability. The bifurcation point

$$p^* = \frac{d + 1}{\kappa}, \tag{4}$$

where the DFS loses stability is referred to as the *epidemic threshold*.

The non-trivial solution corresponding to the *endemic state*, $P_{\mathrm{I}} > 0$, is found by setting the left hand side of Eqs. (1a), (1b) and (2a)–(2f) to zero. We obtain the following steady state relations for the endemic state:

$$P_{\mathrm{SS}} = \left(\frac{d + 1}{p\kappa}\right)(1 - P_{\mathrm{I}}), \tag{5a}$$

$$P_{\mathrm{SI}} = \frac{2}{p\kappa} P_{\mathrm{I}}, \tag{5b}$$

$$P_{\mathrm{II}} = \frac{P_{\mathrm{I}}}{\kappa} + \frac{P_{\mathrm{I}}^2}{p\kappa(1 - P_{\mathrm{I}})}, \tag{5c}$$

$$P_{\widehat{\mathrm{SS}}} = \frac{2d}{p\kappa a} P_{\mathrm{I}}, \tag{5d}$$

$$P_{\widehat{\mathrm{SI}}} = \frac{2d}{p\kappa} P_{\mathrm{I}} + \frac{4d}{p\kappa a} \frac{P_{\mathrm{I}}^2}{1 - P_{\mathrm{I}}}, \tag{5e}$$

$$P_{\widehat{\mathrm{II}}} = \frac{d}{p\kappa}\frac{P_{\mathrm{I}}^2}{1-P_{\mathrm{I}}} + \frac{2d}{p\kappa a}\frac{P_{\mathrm{I}}^3}{(1-P_{\mathrm{I}})^2}. \tag{5f}$$

Using conservation of links, we obtain the following cubic equation in P_{I}:

$$P_{\mathrm{I}}^3 - P_{\mathrm{I}}^2(\kappa+2) + P_{\mathrm{I}}(\kappa+1+A+B) - B = 0, \tag{6}$$

where $A \equiv (2d)/(pa)$ and $B \equiv \kappa - (d+1)/p$. This cubic can be solved to obtain the infection level for parameter values of interest.

At the epidemic threshold, $B = 0$, Eq. (6) takes the form

$$P_{\mathrm{I}}\big(P_{\mathrm{I}}^2 - P_{\mathrm{I}}(\kappa+2) + \kappa + 1 + A\big) = 0.$$

Nonzero solutions are

$$P_{\mathrm{I}} = 1 + \frac{1}{2}\big(\kappa \pm \sqrt{\kappa^2 - 4A}\big), \tag{7}$$

both of which are either imaginary or greater than 1 for positive parameter values. Thus, at the epidemic threshold, there is no solution for $P_{\mathrm{I}} \in (0,1)$, the allowed range of endemic states. Models with rewiring adaptation typically show a backward transcritical bifurcation in the infection rate [6, 19, 24], which leads to bistability. An endemic steady state exists at the epidemic threshold in these models. We have shown that at the epidemic threshold, our model has the disease-free state as its only steady state. We thus argue that our adaptation mechanism of link deactivation and reactivation does not produce bistability. Numerical results described in the next section support this argument and indicate that a forward transcritical bifurcation in infection rate occurs at the epidemic threshold.

Finally, we note that in the absence of adaptation, the equation below is derived by setting $a = d = 0$ and solving Eqs. (1a), (1b) and (2a)–(2f) at the steady state:

$$P_{\mathrm{I}}^2 - P_{\mathrm{I}}(\kappa+1) + (\kappa - 1/p) = 0. \tag{8}$$

4 Results

We next present the results of numerically simulating the adaptive system on an Erdős-Rényi random network [3] and compare the results to those predicted by the steady state of the mean-field theory given by Eqs. (5a)–(5f) and (6). In Fig. 2, we show the steady state value of the fraction of infecteds as a function of infection rate p and deactivation rate d for fixed reactivation rate a. As expected, the levels of infection grow as the infection rate p is increased. Furthermore, increasing deactivation rate d leads to suppression of infection due to decreased number of potential channels of infection transmission. The onset of the endemic state is in good agreement with the mean-field threshold prediction (4), as indicated by the white curve. We note that although Fig. 2 was obtained by averaging over 20 Erdős-Rényi network realizations, the standard deviation of infecteds across networks is less than 1 % of the mean except very close to the threshold where variations are larger. In subsequent figures we present results for only one typical network realization, but the error bars across different realizations would generally be within the plotting resolution.

The results presented in Fig. 3 indicate excellent agreement of the mean-field with the simulations for various parameter values and demonstrate the effects of activation and deactivation on the bifurcation diagrams of fraction of infected nodes versus infection rate. Thus,

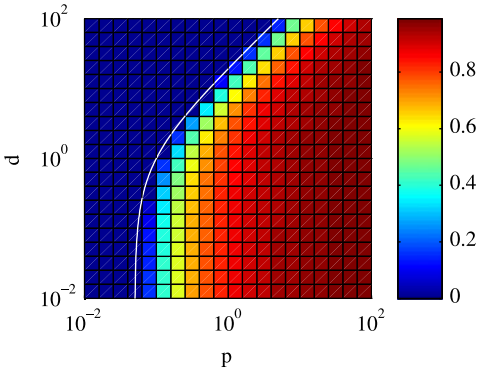

Fig. 2 Density plot of the steady state fraction of infected nodes in the adaptive system, plotted as a function of infection rate, p, and deactivation rate, d, for the reactivation rate $a = 10$. The results of the simulations are averaged over 20 network realizations and 100 time points for each network with 1000 events between each time point. The number of events discarded as transients ranged from 3×10^9 to 10^8 for different d and p values. The *white curve* indicates the location of the threshold as predicted by the mean-field theory in Eq. (4) (Color figure online)

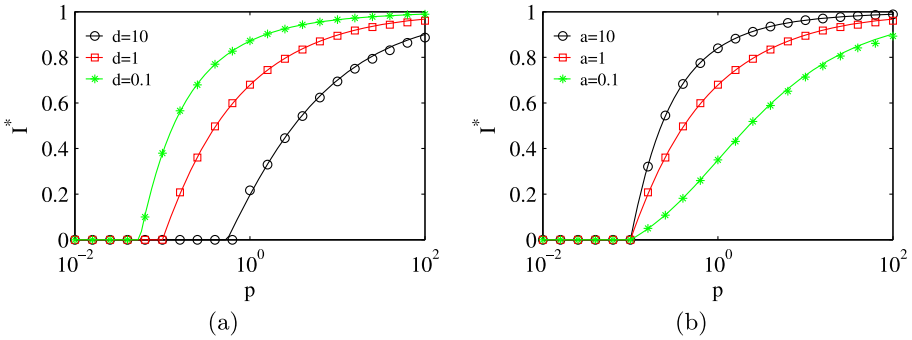

Fig. 3 (**a**) Fraction of infected nodes as a function of infection rate for $a = 1$ and fixed d values. (**b**) Fraction of infected nodes as a function of infection rate for $d = 1$ and fixed a values. *Curves* are mean-field solutions and *symbols* are simulation results. Bifurcation curves were obtained in simulations by sweeping p downward after discarding transients (Color figure online)

in Fig. 3(a), we show that by varying d, we affect the location of the epidemic threshold. Note that this result is also observed in Fig. 2. By contrast, increasing a has no effect on the location of the epidemic threshold as shown in Fig. 3(b), a result that is consistent with the mean-field prediction in Eq. (4). However, as we increase the rate of reactivation, the steady state fraction of infecteds increases, partially negating the effect of deactivation.

In our model, the initial network geometry is not evolving in time. What changes is the active part of the network, via which the disease can be transmitted. The active network geometry evolves due to the interplay between the link deactivation/reactivation and the node status. The effect that adaptation has on the network topology can be observed through the average active degree. For a given infection rate p and reactivation rate a, when the deactivation rate d is zero, the network is fully active and therefore the mean active degree simply equals the mean degree of the network. Figure 4 demonstrates that increasing the deactivation rate leads to the reduction of the active degree of the network and as a consequence

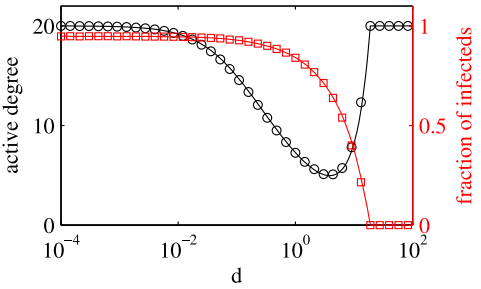

Fig. 4 Dependence of mean active degree of the network on deactivation rate d (*left axis*, *black circles*), as compared to the dependence of the expected fraction of infected nodes on d (*right axis*, *red squares*). The *solid curves* are the corresponding mean-field predictions and *symbols* are simulation results. The simulation results are obtained for $N = 10^5$, $K = 10^6$, $r = 1$, $p = 1$, $a = 10$ after discarding 10^9 number of events (Color figure online)

the reduction in the expected number of infected nodes. However, further increases in the deactivation rate will eventually lead to an increase in the mean active degree, while further reducing the infection level. This suggests that the adaptation mechanism functions in two qualitatively different regimes, which we attribute to the presence of slow and non-slow network dynamics regimes.

First, we consider the behavior of the system at the steady state in the limit of slow network dynamics, where deactivation and reactivation processes are much slower than the infection transmission. The steady state solution of the mean-field equations (5a)–(5f) suggests that the non-trivial regime of the slow network dynamics is given by the limit of $d, a \to 0$ with $d/a = c$, for a constant c. In this limit, we study the disease spreading on a static network, frozen with only some fraction of its links being active.

The limiting behavior of our adaptive system in steady state is captured by taking the corresponding limit of the steady state solution of the mean-field equations (5a)–(5f). Thus, in the limit under consideration, the terms proportional to d drop out, while the terms proportional to d/a survive, yielding the following expected fraction of deactivated and active links in the system, respectively:

$$P^*_{\text{deactivated}} \equiv \lim_{\substack{d,a\to 0 \\ d/a=c}} (P_{\widehat{\text{SS}}} + P_{\widehat{\text{SI}}} + P_{\widehat{\text{II}}}) = \frac{2cP_{\text{I}}}{p\kappa(1-P_{\text{I}})^2}, \tag{9}$$

$$P^*_{\text{active}} \equiv 1 - P^*_{\text{deactivated}} = \left(1 - \frac{2cP_{\text{I}}}{p\kappa(1-P_{\text{I}})^2}\right). \tag{10}$$

Solving Eq. (10) for c and substituting the result into the corresponding limit of Eq. (6) (i.e., $A = 2c/p$, $B = \kappa - 1/p$), we see that P_{I} satisfies the following equation:

$$(P_{\text{I}} - 1)\left(P_{\text{I}}^2 - P_{\text{I}}\left(\kappa P^*_{\text{active}} + 1\right) + \kappa P^*_{\text{active}} - \frac{1}{p}\right) = 0.$$

Since the solution $P_{\text{I}} = 1$, where all the nodes are infected, is not a physically possible steady state, the fraction of infected nodes P_{I} must satisfy the following equation:

$$P_{\text{I}}^2 - P_{\text{I}}\left(\kappa P^*_{\text{active}} + 1\right) + \kappa P^*_{\text{active}} - \frac{1}{p} = 0, \tag{11}$$

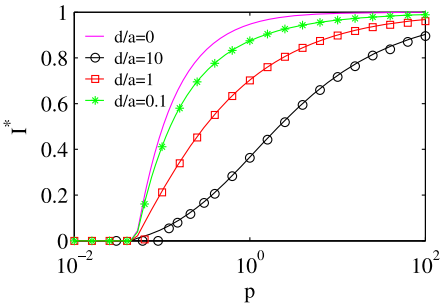

Fig. 5 Comparison of simulation results for adaptive networks with mean-field solutions for a static network (SMF), where the mean degree in the static network is matched with the active degree in the adaptive one. *Curves*: mean-field solution of epidemic model on static network. *Symbols*: simulation results of epidemic model on adaptive network with $d = 10^{-2}$. Case $d/a = 0$ represents original static network with all links active. The simulation results for $d/a = 10$ and $p < 1$ are obtained for $N = 10^5$ and $K = 10^6$ (Color figure online)

which, as shown in Eq. (8), is precisely the equation that describes the steady state infection level in a static network with mean degree $\kappa P^*_{\text{active}}$. Note that P^*_{active} depends on all of the system parameters and the value of P_{I}, with the dependence on the deactivation and reactivation rates only via the ratio of those rates.

The significance of the above is that in the slow network limit, the function of adaptation is merely to suppress the mean active degree of the nodes. In other words, the adaptation reduces the mean number of potential channels for the disease transmission, regardless of the status of the nodes at the end of a channel. Figure 5 shows that the fraction of infected nodes in the system, when the adaptation rates are much slower than the rates of the disease dynamics, is well approximated by the mean-field theory for a static network with mean degree corresponding to the mean active degree, $\kappa P^*_{\text{active}}$. Furthermore, we can see that as c approaches zero, the system approaches the mean-field solution for the network without adaptation. Thus, given the active degree of the nodes in the network, possibly measured from the simulations, we can use the *static* network *mean-field* description with the corresponding mean degree (SMF) to analyze our system in this regime. Away from the limit where a and d approach zero the assumption that the disease spreads on a static network is no longer valid. In this regime the network changes on a time scale comparable to the time scale of the disease dynamics, and the nature of the adaptation mechanism becomes more complex. In Fig. 6, we emphasize the difference between the SMF solution and the simulation results. The overestimation of the infection levels by the static mean-field approach demonstrates that, in the fast network dynamics regime, the adaptation mechanism is more effective than merely mean active degree reduction.

Now we turn to investigating how the adaptive network deviates from the static network with corresponding mean degree. Figure 7(a) demonstrates this deviation as we increase the adaptation parameters a and d, while keeping their ratio fixed. As we previously observed, the SMF theory makes excellent predictions about the infection levels when the network dynamics is slow; however, as the deactivation rate becomes either comparable to or greater than either the recovery or the infection rate, the SMF significantly overestimates the infection level. This is well explained by the steady state solution in Eqs. (5a)–(5f), where we observe that as d is increased, the $d = 0$ assumption made when deriving the SMF is no longer valid. We quantify effects of the adaptation by looking at the local neighborhood of

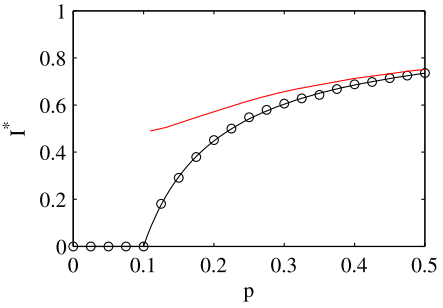

Fig. 6 Fraction of infected nodes as a function of infection rate p in the fast adaptation regime. *Black curve*: mean-field solution for model with adaptation. *Red curve*: SMF solution. *Symbols*: simulation results for adaptive epidemic model for $d = 1$ and $a = 10$ (Color figure online)

susceptible and infected nodes using the metric

$$\frac{\langle\kappa\rangle_{SI}}{\langle\kappa\rangle_{II}} = \frac{P_{SI}/(2P_{SS} + P_{SI})}{2P_{II}/(P_{SI} + 2P_{II})},$$

where $\langle\kappa\rangle_{SI}$ is the fraction of actively connected neighbors of a susceptible node that are infected, and similarly $\langle\kappa\rangle_{II}$ is the fraction of actively connected neighbors of an infected node that are infected. As shown in Fig. 7(b), at rapid deactivation rates where the SMF no longer holds, the expected fraction of infected nodes in the neighborhood of a susceptible node becomes smaller than this fraction in the neighborhood of an infected node. In other words, the mechanism of adaptation, in addition to mean degree reduction, reduces the exposure of susceptible nodes to the infected ones. The full mean-field theory for the adaptive network, given by Eq. (6) and associated equations, continues to hold in the fast network dynamics regime.

5 Conclusions

We studied a susceptible-infected-susceptible model on an adaptive network with a new adaptation mechanism. In our model, a susceptible node temporarily deactivates its links to

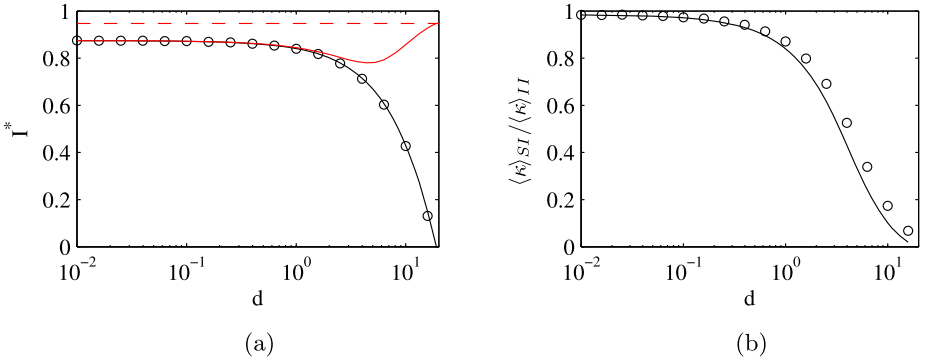

Fig. 7 (**a**) Fraction of infected nodes as a function of deactivation rate d. (**b**) $\langle\kappa\rangle_{SI}/\langle\kappa\rangle_{II}$ as a function of d, where $\langle\kappa\rangle_{SI}$ is the fraction of infected neighbors of a susceptible node and similarly, $\langle\kappa\rangle_{II}$ is the fraction of infected neighbors of an infected node. *Black solid curve*: mean-field solution for model with adaptation, *Red solid curve*: mean-field solution for static model with corresponding mean degree (SMF), *Red dashed curve*: mean-field solution for static model with all links active ($\kappa = 20$), *symbols*: simulation results for network with adaptation where $d/a = 0.1$ and $p = 1$ (Color figure online)

infected nodes. It reactivates the previously deactivated links to its neighbors once they have recovered. Although the active degree of the node is evolving, its original set of neighbors is preserved, which we believe is a more realistic adaptation mechanism than models that allow nodes to form connections anywhere in the network.

We derived and analyzed a system of mean-field equations based on a moment closure approximation. Solutions of the mean-field equations were compared with simulations of the full system on an Erdős-Rényi random network and were in good agreement. An expression for the epidemic threshold was obtained. In contrast to models with a rewiring mechanism for infection avoidance [6, 16, 19, 24], our model does not display bistable solutions. We observe in numerical simulations a forward transcritical bifurcation as the infection rate is increased past the threshold, and we argue from the mean-field equations that a backward transcritical bifurcation and bistability cannot occur.

We studied the infection level and geometry of the active subnetwork as a function of disease and adaptation parameters. The epidemic threshold depended on the link deactivation rate but not the reactivation rate. However, slowing the reactivation decreases the steady state infection level. The average node degree in the active subnetwork was found to depend non-monotonically on the link deactivation rate. While initially counterintuitive, this result can be understood by realizing that the epidemic is better controlled at high deactivation rates, and numbers of infectives and SI links are lower, so the total amount of link deactivation is less even though the per link deactivation rate is higher. This observation suggests that very rapid social adaptation that more effectively controls disease spread can lead to less disruption of a social network than slower adaptation would.

The adaptation mechanism in our model has two methods by which it reduces the spread of infection. Which method is most pronounced depends on the speed of the network dynamics relative to the disease dynamics. First, adaptation reduces the average active degree of the network. When deactivation and reactivation are slow, nodes change their state frequently and the infection spreads quickly on the remaining active links. The reduction in the active degree matters more than which specific links are deactivated. We compared the steady state results of our model with an SIS model on a static network having the same degree as the active degree in our model. In the regime where the dynamics of the network is much slower than the disease dynamics, the infection level in our model is very close to that in the corresponding static network. However, when both the network dynamics and the disease dynamics have comparable time scales, we observed a difference between our model and the static network model with the same active degree. Since the deactivation mechanism in our model is preferential, a susceptible node deactivates its links specifically to infected nodes. Thus, in this regime, infection spread is suppressed to a greater extent than in the corresponding static network.

Here we have focused on an Erdős-Rényi random network. However, more realistic network geometries can be selected for the overarching static network. In contrast to rewiring networks, in which rewiring rules must be carefully selected to preserve desired aspects of the geometry such as community structure [22], the network structure is automatically maintained. In a future work, we will consider the effects of this adaptation mechanism on a scale-free network.

Another area for future study is the role of fluctuations in the different parameter regimes. When the network dynamics is fast, a node's active degree decreases drastically while it is infected and increases while it is susceptible. However, the active degree fluctuates much less when the network dynamics is slow. Our simulations indicate that these fluctuations do not significantly affect the overall infection level in the system, but they may influence aspects of the active network geometry such as degree distributions.

Acknowledgements This work was supported by the Army Research Office, Air Force Office of Scientific Research, and by Award Number R01GM090204 from the National Institute of General Medical Sciences. The content is solely the responsibility of the authors and does not necessarily represent the official views of the National Institute of General Medical Sciences or the National Institutes of Health.

References

1. Albert, R., Barabási, A.L.: Statistical mechanics of complex networks. Rev. Mod. Phys. **74**, 47–97 (2002)
2. Anderson, R.M., May, R.M.: Infectious Diseases of Humans: Dynamics and Control. Oxford University Press, Oxford (1992)
3. Erdős, P., Rényi, A.: On random graphs. Publ. Math. (Debr.) **6**, 290–297 (1959)
4. Gillespie, D.: Exact stochastic simulation of coupled chemical reactions. J. Phys. Chem. **81**(25), 2340–2361 (1977)
5. Gross, T., Blasius, B.: Adaptive coevolutionary networks: a review. J. R. Soc. Interface **5**(20), 259–271 (2008)
6. Gross, T., D'Lima, C.J.D., Blasius, B.: Epidemic dynamics on an adaptive network. Phys. Rev. Lett. **96**, 208701 (2006)
7. Jolad, S., Liu, W., Schmittmann, B., Zia, R.K.P.: Epidemic spreading on preferred degree adaptive networks. arXiv:1109.5440v1 (2011)
8. Keeling, M.J., Eames, K.: Networks and epidemic models. J. R. Soc. Interface **2**(4), 295–307 (2005)
9. Keeling, M.J., Rand, D.A., Morris, A.J.: Correlation models for childhood epidemics. Proc. R. Soc. Lond. B, Biol. Sci. **264**(1385), 1149–1156 (1997)
10. Kiss, I.Z., Berthouze, L., Taylor, T.J., Simon, P.L.: Modelling approaches for simple dynamic networks and applications to disease transmission models. Proc. R. Soc. A, Math. Phys. Eng. Sci. **468**(2141), 1332–1355 (2012)
11. May, R.M., Lloyd, A.: Infection dynamics on scale-free networks. Phys. Rev. E **64**(6), 066112 (2001)
12. Newman, M.E.J.: Spread of epidemic disease on networks. Phys. Rev. E **66**(1), 016128 (2002)
13. Newman, M.E.J.: The structure and function of complex networks. SIAM Rev. **45**(2), 167–256 (2003)
14. Pastor-Satorras, R., Vespignani, A.: Epidemic dynamics and endemic states in complex networks. Phys. Rev. E **63**, 066117 (2001)
15. Pastor-Satorras, R., Vespignani, A.: Epidemic spreading in scale-free networks. Phys. Rev. Lett. **86**(14), 3200–3203 (2001)
16. Risau-Gusman, S., Zanette, D.: Contact switching as a control strategy for epidemic outbreaks. J. Theor. Biol. **257**(1), 52–60 (2009)
17. Schwartz, I., Shaw, L.: Rewiring for adaptation. Physics **3**, 17 (2010)
18. Schwarzkopf, Y., Rákos, A., Mukamel, D.: Epidemic spreading in evolving networks. Phys. Rev. E **82**(3), 036112 (2010)
19. Shaw, L., Schwartz, I.B.: Fluctuating epidemics on adaptive networks. Phys. Rev. E **77**(6), 066101 (2008)
20. Shkarayev, M.S., Schwartz, I.B., Shaw, L.B.: Recruitment dynamics in adaptive social networks. arXiv:1111.0964 (2012)
21. Taylor, M., Taylor, T., Kiss, I.: Epidemic threshold and control in a dynamic network. Phys. Rev. E **85**(1), 016103 (2012)
22. Tunc, I., Shaw, L.B.: Effects of community structure on epidemic spread in an adaptive network. arXiv:1212.3229
23. Valdez, L.D., Macri, P.A., Braunstein, L.A.: Intermittent social distancing strategy for epidemic control. Phys. Rev. E **85**, 036108 (2012)
24. Zanette, D.: Infection spreading in a population with evolving contacts. J. Biol. Phys. **34**(1), 135–148 (2008)
25. Zhou, J., Xiao, G., Cheong, S., Fu, X., Wong, L.: Epidemic reemergence in adaptive complex networks, pp. 1–8 (2012). arXiv:1203.0366v1